Imaging Stroke Through the Skull Using Ultrasound Tomography

Trevor Mitcham[1], Rehman Ali[1], Derrek Schartz[1], Redi Rahmani[4], Melanie Singh[2], Matthew Bender[3], Edward Vates[3], Neb Duric[1,2]

[1]University of Rochester, Department of Imaging Sciences, Rochester, NY, USA.

[2]University of Rochester, Department of Biomedical Engineering, Rochester, NY, USA.

[3]University of Rochester, Department of Neurosurgery, Rochester, NY, USA.

[4]Barrow Neurological Institute, Department of Neurosurgery, Phoenix, AZ.

Abstract

Stroke is a significant cause of mortality and disability in America. Due to differences in the treatment of ischemic and hemorrhagic stroke, imaging must be performed before administration of therapeutic medication. Unfortunately, the current standard imaging methods, namely CT and MRI, require specialized locations and staff, which can induce delays in triage, and therefore, treatment time. Recent work suggests that ultrasound tomography (UST) is capable of imaging *in vivo* tissue properties and may have potential as a diagnostic tool during stroke treatment which could be performed at the point of injury rather than at a local hospital. In this work, we investigate the feasibility of using UST imaging to image the brain via *in silico*, *in vitro*, and *ex vivo* studies. The results of this work indicate some of the challenges which must be overcome to effectively image *in vivo* stroke patients.

Background

Per the American Heart Association, stroke is fifth leading cause of death in the United States and the leading cause of disability[1]. The majority of strokes are due to clots that block blood supply to the brain (i.e., ischemic stroke), and imaging is key to triaging and planning treatment[1,2]. Even with optimal treatment, stroke survivors often suffer from severe long-term impairment and increased mortality[3].

Currently, imaging is a key step in triaging and planning stroke treatment. Standard clinical imaging modalities currently include imaging with CT or MRI to rule out hemorrhage, both of which require transportation of the patient to a nearby hospital. In practice, the time needed to transport the patient to a hospital and perform the imaging are major factors that define current door to needle time (i.e., the delay in administration of therapeutic medication to prevent further damage)[3]. Therefore, the greatest barrier to reducing this time is the lack of a triaging method that can be deployed *before* the patient is transported to the ER.

To that end, some hospitals use mobile CT ambulances or Mobile Stroke Units[4]. However, these options are not widely available, especially in rural and under-resourced areas owing to high capital and maintenance expenses[5]. Therefore, point-of-injury brain imaging for rapid stroke assessment and triaging is a major unmet need. Ideally, a portable, low-cost device that can be carried in a typical ambulance and used at the site (e.g., the patient's home), would make early interventions widely available *thereby minimizing delays in treatment and positively impacting stroke recovery*[6].

Ultrasound tomography (UST) has emerged as a clinical modality capable of quantitatively imaging *in vivo* tissue parameters which may provide improved or expedited imaging through the skull as compared to current imaging modalities[7]. Additionally, US imaging through the skull has become a

Medical Imaging 2024: Ultrasonic Imaging and Tomography, edited by Christian Boehm, Nick Bottenus,
Proc. of SPIE Vol. 12932, 129320J · © 2024 SPIE · 1605-7422
doi: 10.1117/12.3006595

topic of increased interest in recent years[8]. Therefore, in this work, we investigate the feasibility of using UST to characterize stroke utilizing simulation data, *in vitro* phantoms, and *ex vivo* tissue samples.

Methods

A) K-Wave Simulation Images

Initial *in silico* experiments utilized the MATLAB toolbox k-wave to simulate ultrasonic propagation through a brain hemorrhage model[9]. A normal head CT scan[10] is used to derive the model via the piecewise fitting of Hounsfield Units to density and sound speed[11], and a subarachnoid or intercranial hemorrhage inclusion is added to reflect literature values of whole blood[12]. The ultrasound imaging simulation uses a broadband low frequency ring transducer (1024 elements, 22cm diameter, 1MHz center frequency, and 75% BW) to produce RF data. Randomly distributed noise (±1 standard deviation from baseline) is added to the RF data. Reconstructed images are achieved through our existing full waveform inversion (FWI) algorithms, and the reconstructed images were then compared to the "truth" image (Fig 1A, B), to benchmark ideal UST image quality and define limitations. To briefly describe the FWI algorithm, the 2D Helmholtz equation is solved using finite difference methods, and this is compared to measured data at the ring array at discrete frequencies. For FWI reconstruction, the initial model utilized a two-component medium composed of a 1.8 mm thick skull model derived from the outer boundary of the reflection image (2000 m/s sound speed), with the remaining medium modeled as water (1500 m/s sound speed). The FWI process is repeated every 10 kHz from 50 kHz to 700 kHz with three iterations per frequency. Full details of the FWI reconstruction algorithm can be found in[13].

B) Image acquisition and Reconstruction

For all physical experiments, UST imaging was performed on a Verasonics Vantage 256 system (Verasonics Inc., Kirkland, WA) with a 1024-element ring array (Fig. 1C; TransducerWorks, LLC, Centre Hall, PA; 3 MHz center frequency, 1-4 MHz Bandwidth)[14]. The transducer was driven at 700 kHz to ensure appropriate low frequency content in the waveform to begin full waveform inversion image reconstruction[13]. For all UST images in this work, reconstruction was performed using FWI techniques (350-900 kHz, 50 kHz step size) to generate sound speed and attenuation images, while traditional reflection images were also generated to aid with localization of the features.

C) In vitro Phantom imaging and characterization

After validating that *in silico* images generated acceptable images, a human replica skull (Skulls Unlimited Inc., Oklahoma City, OK) was used to demonstrate our current ability to image through bone-mimicking material (Fig. 1 C). The skull phantom was first filled with an 8% gelatin mixture (Sigma-Aldrich, Inc., St. Louis, MO) along with two inclusions which were filled with a mixture of 8% gelatin and 20% isopropyl alcohol to create high sound speed imaging targets (i.e., ~1600 m/s; Fig. 1 D)[15]. UST images were taken of a representative cross-section of the phantom using the standard sequence described in (B).

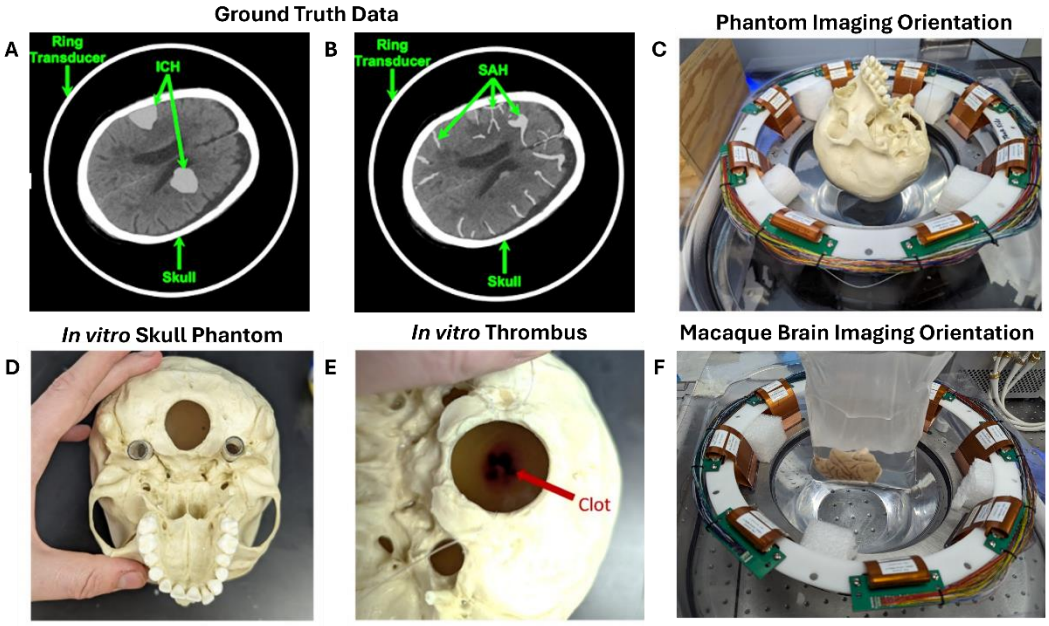

Figure 1: Figure demonstrating experimental work. A) Ground truth model for *in silico* imaging with intracranial hemorrhage. B) Ground truth model for *in silico* imaging with subarachnoid hemorrhage. C) Imaging setup for all experiments using the *in vitro* skull phantom. D) *In vitro* phantom with molds cast for high sound speed inclusions. E) *Ex vivo* thrombus inserted into the *in vitro* skull phantom. F). Preserved macaque brain within the 1024-element ring array transducer.

D) In vitro hemorrhage characterization

Next, the same skull-mimicking phantom was utilized to image a simulated cerebral hemorrhage. The same brain-tissue-mimicking background was used to fill the replica skull, and three negative molds were cast within the gelatin to provide wells which could be used to simulate bleeding. One large well (3 cm diameter) and two small wells (1 cm diameter) were injected with whole *ex vivo* blood and subsequently imaged with UST using the previously stated imaging parameters described in (B).

E) In vitro thrombus characterization

Finally, an *ex vivo* blood clot was sourced and then embedded within the same brain-tissue-mimicking gelatin mixture within the skull phantom (Fig. 1E) to determine the feasibility of resolving a clot through the skull with both sound speed and reflection imaging. UST images were taken of a representative cross-section of the phantom and FWI reconstruction was performed with standard parameters as listed previously in (B).

F) Ex Vivo Characterization of Intact Brain

The final experiment was to image an intact macaque brain which had been preserved in 10% formalin solution. The brain was rehydrated in 10mM PBS (pH7.4) for two weeks prior to imaging to reduce tissue stiffness. For imaging, the sample was placed inside a transparent plastic bag filled with 10mM PBS solution, and then imaged at multiple elevational slices to characterize the acoustic properties throughout the full volume to provide a baseline image quality for brain tissue moving forward (Fig.

1E). One additional image was acquired of the preserved brain sample within the skull-mimicking phantom in order to show the effects of the skull phantom on the anatomical features.

Results

A) *In silico* imaging results

K-Wave simulations support our hypothesis that UST is capable of imaging pathologies through the skull, providing a roadmap for experimental work (Fig. 2). Artifacts due to cycle skipping and high sound speed contrast are minimized when beginning reconstruction at 50 kHz, while anatomical features of the brain as well as both intracranial (Fig. 2A) and subarachnoid (Fig. 2B) hemorrhages can be visualized clearly within the simulated imaging datasets.

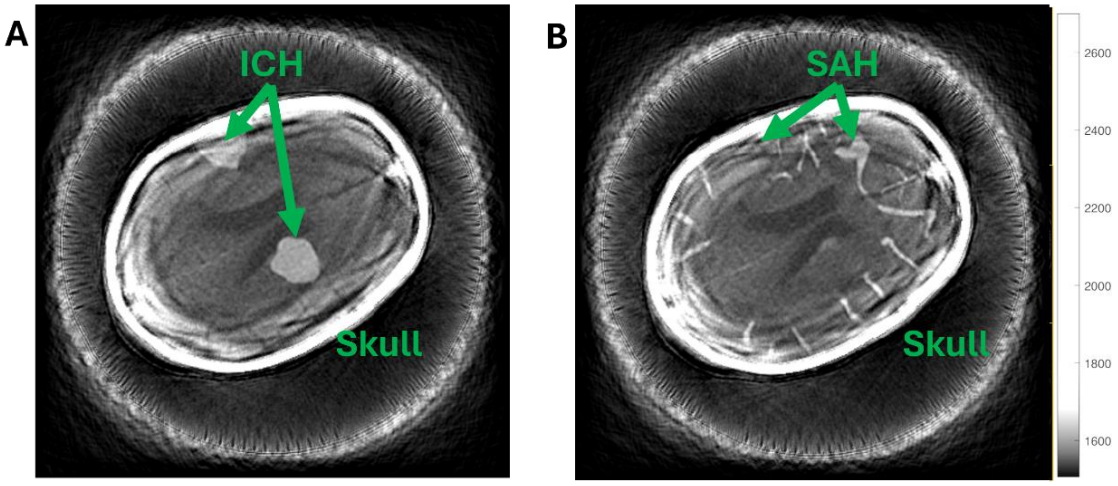

Figure 2: A) Image of the K-wave simulated data propagated through the medium in (1A) containing intracranial hemorrhages were reconstructed using FWI reconstruction. B) Image of the K-wave simulated data propagated through the medium in (1B) containing subarachnoid hemorrhages were reconstructed using FWI reconstruction

B) In vitro phantom characterization results

Using our current hardware setup, we successfully imaged the high sound speed inclusions through the replica skull, albeit with cycle skipping due to the relatively high-frequency content of the waveform (Fig. 3). Reflection images also show image contrast between the inclusions and the background medium.

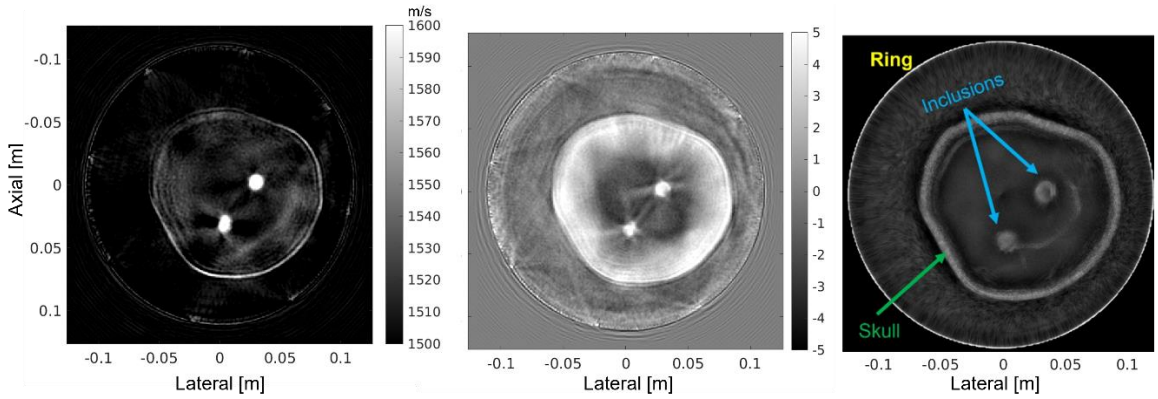

Figure 3: A) FWI sound speed image of *in vitro* phantom with two high sound speed inclusions visualized despite cycle skipping artifacts. B) Attenuation and C) Reflection image of the same phantom.

C) *In vitro hemorrhage characterization results*

Despite the presence of artifacts, all three hemorrhages could be visualized within the skull-mimicking phantom in sound speed, attenuation, and reflection images (Fig. 4). The background gelatin medium showed an average sound speed value of 1521 ± 9 m/s, while hemorrhages showed an average sound speed of 1564 ± 5 m/s.

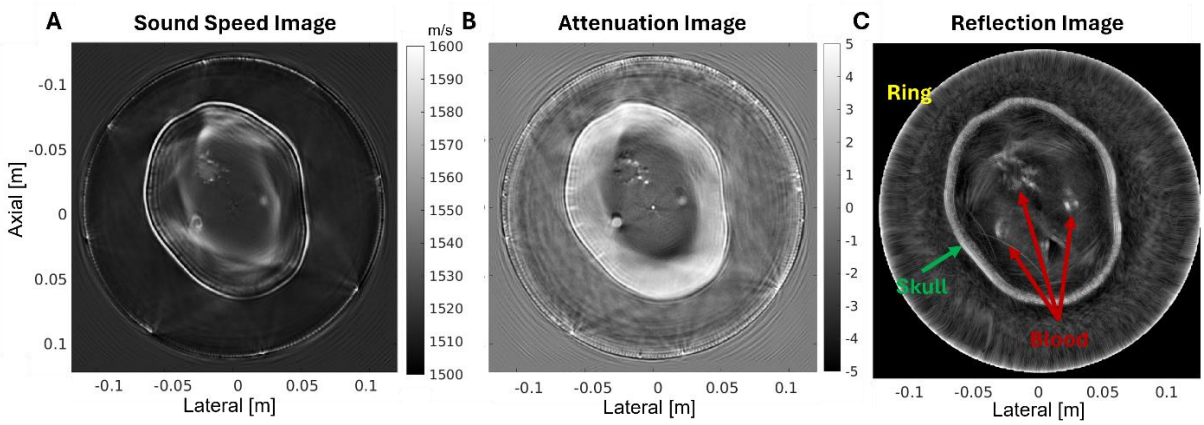

Figure 4: *In* vitro hemorrhage phantom with three *ex* vivo blood inclusions in A) FWI-based sound speed, B) FWI-based attenuation, and C) reflection images showing annotation of the phantom features.

D) *In vitro* thrombus characterization results

Finally, we successfully visualized a retrieved human blood clot within a replica skull, thereby defining the baseline challenges (i.e., cycle skipping, skull mapping) that will guide future technique development. (Fig. 5). Despite cycle skipping artifacts, the thrombus can be visualized with a sound speed of 1570 m/s.

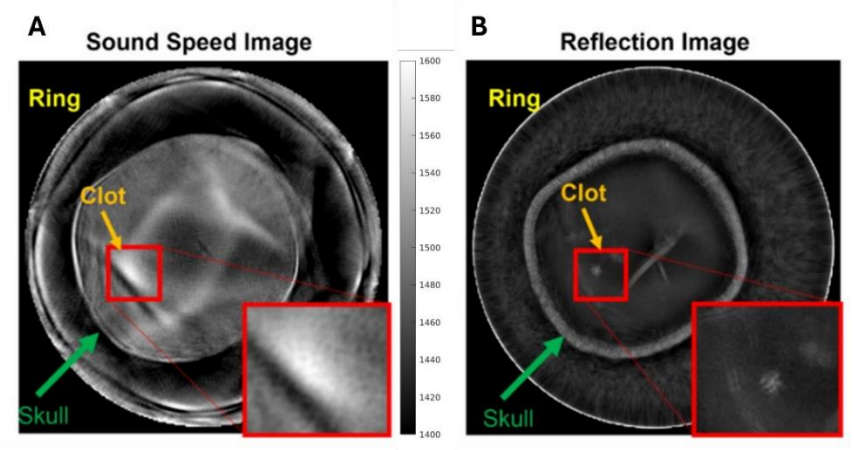

Figure 5: A) Sound speed image of a representative slice showing the skull boundary as well as the clot. B) Matched reflection image to (A), validating the location of the clot as well as the skull boundary.

E) Ex vivo brain characterization results

Multiple anatomic features, including the interhemispheric fissure, sylvian fissure, ventricles, and the brain stem, can all be visualized in sound speed and reflection images (Fig. 6)[16,17]. Sound speed values within the preserved brain ranged from 1500-1580 m/s, which is approximately consistent with the increased stiffness expected in preserved tissue[18,19]. Within the skull phantom, the brain sample could still be resolved in all three reconstructions, and the interhemispheric fissure can be clearly visualized.

Discussion

In this work, we present validation that UST imaging can detect multiple hemorrhage types in a realistic simulation environment, while also detecting generalized regions of high sound speed, *ex vivo* whole blood, and *ex* vivo blood clots within a tissue-mimicking phantom environment in real experimental data. Additionally, we characterize our ability to visualize the anatomy of a healthy brain without a skull-mimicking material to demonstrate the ultimate potential of this technique. These results show that UST imaging is feasible through a skull-mimicking phantom, although further work is needed to optimize the imaging and reconstruction due to the presence of significant artifacts.

In vitro high sound speed inclusions within the skull phantom were visible in all three reconstructions (i.e., sound speed, attenuation, and reflection); however, the presence of artifacts in both reflection (due to refraction) and sound speed (due to cycle skipping) images demonstrate the need for improvement. *Ex vivo* whole blood was also visualized very clearly across all three reconstructions with relatively few artifacts present. Finally, retrieved *ex vivo* blood clots displayed contrast in all three imaging reconstructions performed (i.e., reflection, sound speed, and attenuation), and sound speed values recorded were consistent with literature values at similar temperatures and clot ages[20]. While all three skull phantom experiments showed cycle skipping and refraction artifacts, the artifacts appear differently across all three experiments. This can likely be attributed to improvements in the FWI algorithm as well as imaging the three phantoms at different skull positions, allowing for an

optimal acoustic window in the hemorrhage phantom, which will need to be investigated further in subsequent work.

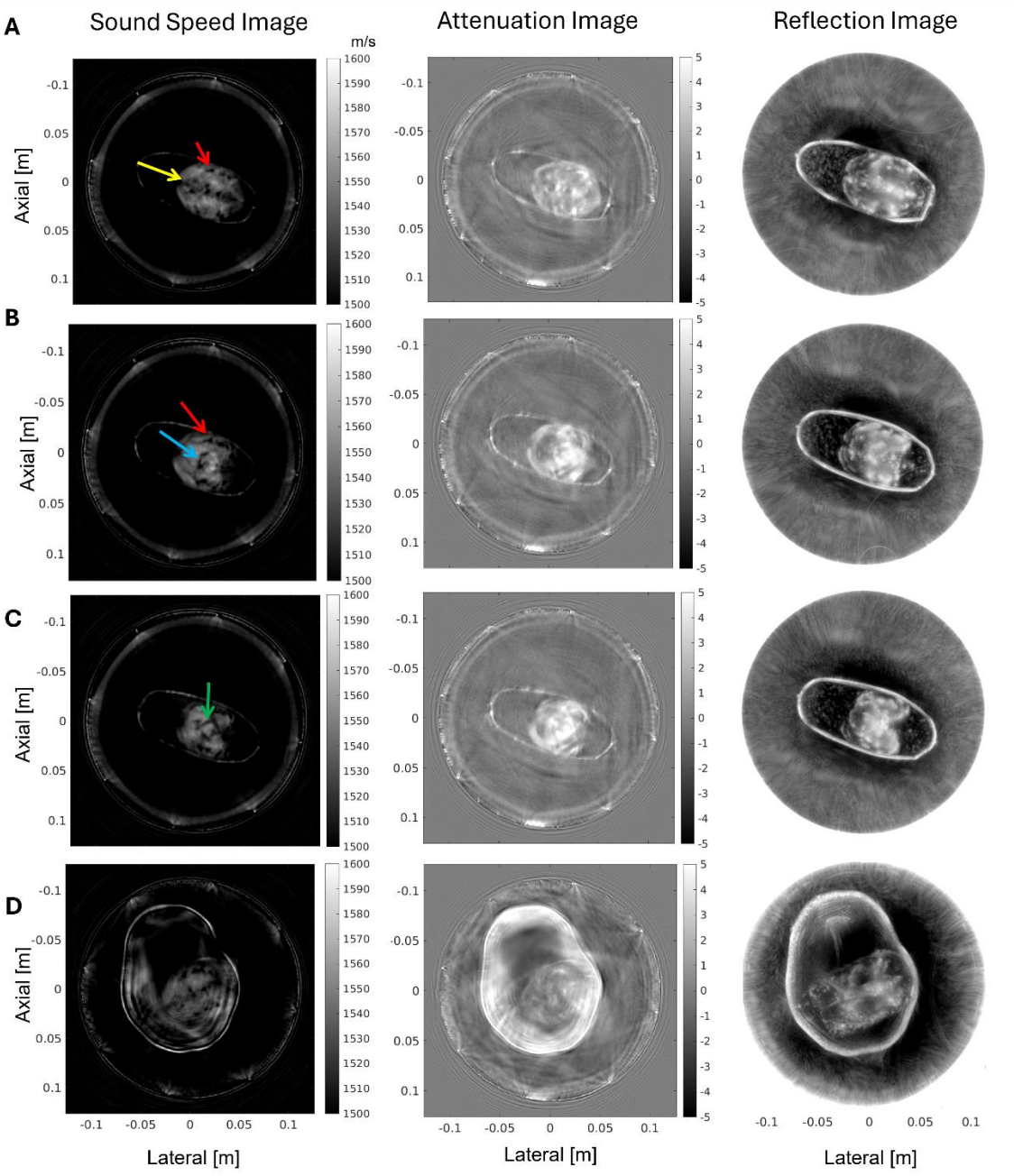

Figure 6: A) Image of a cross-section of the preserved macaque brain, in which the interhemispheric fissure (yellow) and sylvian fissure (red) are visible in sound speed, attenuation, and reflection imaging. B) Image of a cross-section of the preserved macaque brain, in which the sylvian fissure (red) and ventricles (cyan) are visible in sound speed, attenuation, and reflection imaging. C) Image of a cross-section of the preserved macaque brain, in which the brain stem (green) is visible in sound speed, attenuation, and reflection imaging D) Image of a cross-section of the macaque brain within the skull-mimicking phantom, in which the brain can be seen with the interhemispheric fissure in the bottom of the skull

In addition to the phantom experiments, the fixed macaque brain provides insight into the ultimate goal of this work. In all three image reconstructions, multiple anatomic features can be clearly visualized, demonstrating that UST imaging can provide sufficient detail to differentiate healthy and diseased tissue in the event of a stroke. While some features (e.g., interhemispheric fissure) can still be distinguished within the skull-mimicking phantom, the artifacts generally degrade the image quality and mask important anatomic landmarks, which demonstrated the importance of further developing our imaging technique to overcome the artifacts visualized in the phantom experiments.

The artifacts present in this work can be overcome by addressing two sets of issues that can be loosely grouped into hardware and software concerns. Hardware concerns which must be addressed include low signal to noise ratio (SNR) at our desired imaging frequencies (i..e, sub-600 kHz levels), and a complete lack of signal at sub-300 kHz levels, leading to cycle skipping artifacts[13]. As the skull attenuates ultrasound waves significantly more than soft tissue, additional techniques such as virtual sources may also be investigated in order to improve SNR in transmission imaging. Additionally, starting FWI reconstruction at lower frequencies can help to overcome cycle skipping artifacts in imaging samples with high sound speed discontinuities as we expect to see with the skull. Software concerns include investigation of adaptive waveform inversion[21] and the introduction of a two-component model[22] in order to help generate additional low frequency content and provide an accurate starting mode, respectively.

Conclusions

This work shows that UST imaging is feasible through a skull-mimicking phantom for a variety of targets. Simulations of realistic hemorrhages, as well as *in vitro* and *ex vivo* targets could all be visualized in sound speed images despite the presence of cycle skipping artifacts. Additionally, an intact animal brain sample was imaged to demonstrate our current ability to visualize anatomical features within the brain in order to guide future development of this work.

Acknowledgments

We would like to acknowledge clinical insight provided by Dr. Deborah Rubens, we would like to thank Dr. Madalina Tivarus and Brenna Harris for providing skull CT datasets for our use, and we would also like to thank Drs. Allan Johnson. Yi Qi, and Stephanie Blocker from Duke University for providing the preserved Macaque brain sample for imaging.

References

1. Heart Disease and Stroke Statistics—2023 Update: A Report From the American Heart Association | Circulation. https://www.ahajournals.org/doi/full/10.1161/CIR.0000000000001123.
2. Provost, C. *et al.* Magnetic Resonance Imaging or Computed Tomography Before Treatment in Acute Ischemic Stroke. *Stroke* **50**, 659–664 (2019).
3. Mendez, B. *et al.* Direct Transfer to Angio-Suite to Reduce Workflow Times and Increase Favorable Clinical Outcome. *Stroke* **49**, 2723–2727 (2018).
4. Walter, S. *et al.* Diagnosis and treatment of patients with stroke in a mobile stroke unit versus in hospital: a randomised controlled trial. *Lancet Neurol.* **11**, 397–404 (2012).
5. Fassbender, K. *et al.* Impact of mobile stroke units. *J. Neurol. Neurosurg. Psychiatry* **92**, 815–822 (2021).

6. Mitcham, T. *et al.* Feasibility of Imaging Ischemic Stroke Through the Skull Using Ultrasound Tomography. in *2023 IEEE International Ultrasonics Symposium (IUS)* 1–3 (2023). doi:10.1109/IUS51837.2023.10308116.
7. Duric, N. *et al.* Breast ultrasound tomography: bridging the gap to clinical practice. in *Medical Imaging 2012: Ultrasonic Imaging, Tomography, and Therapy* vol. 8320 205–213 (SPIE, 2012).
8. Riis, T. S., Webb, T. D. & Kubanek, J. Acoustic properties across the human skull. *Ultrasonics* **119**, 106591 (2022).
9. k-Wave: MATLAB toolbox for the simulation and reconstruction of photoacoustic wave fields. https://www.spiedigitallibrary.org/journals/journal-of-biomedical-optics/volume-15/issue-2/021314/k-Wave--MATLAB-toolbox-for-the-simulation-and-reconstruction/10.1117/1.3360308.full.
10. Hssayeni, M. Computed Tomography Images for Intracranial Hemorrhage Detection and Segmentation. PhysioNet https://doi.org/10.13026/4NAE-ZG36.
11. Webb, T. D. *et al.* Measurements of the Relationship Between CT Hounsfield Units and Acoustic Velocity and How It Changes With Photon Energy and Reconstruction Method. *IEEE Trans. Ultrason. Ferroelectr. Freq. Control* **65**, 1111–1124 (2018).
12. Mast, T. D. Empirical relationships between acoustic parameters in human soft tissues. *Acoust. Res. Lett. Online* **1**, 37–42 (2000).
13. Ali, R., Mitcham, T. & Duric, N. Impact of starting model on waveform inversion in ultrasound tomography. in *Medical Imaging 2023: Ultrasonic Imaging and Tomography* vol. 12470 89–98 (SPIE, 2023).
14. Acoustic tomography: Promise versus reality | IEEE Conference Publication | IEEE Xplore. https://ieeexplore.ieee.org/abstract/document/6293747/.
15. Tissue-mimicking phantoms for photoacoustic and ultrasonic imaging. https://opg.optica.org/boe/fulltext.cfm?uri=boe-2-11-3193&id=224004.
16. Rushmore, R. J. *et al.* MRI-based Parcellation and Morphometry of the Individual Rhesus Monkey Brain: the macaque Harvard-Oxford Atlas (mHOA), a translational system referencing a standardized ontology. *Brain Imaging Behav.* **15**, 1589–1621 (2021).
17. Calabrese, E. *et al.* A diffusion tensor MRI atlas of the postmortem rhesus macaque brain. *NeuroImage* **117**, 408–416 (2015).
18. Kremkau, F. W., Barnes, R. W. & McGraw, C. P. Ultrasonic attenuation and propagation speed in normal human brain. *J. Acoust. Soc. Am.* **70**, 29–38 (1981).
19. Tamura, K. *et al.* Alteration of speed-of-sound by fixatives and tissue processing methods in scanning acoustic microscopy. *Front. Phys.* **11**, (2023).
20. Nahirnyak, V. M., Yoon, S. W. & Holland, C. K. Acousto-mechanical and thermal properties of clotted blooda). *J. Acoust. Soc. Am.* **119**, 3766–3772 (2006).
21. Adaptive waveform inversion: Theory | GEOPHYSICS. https://library.seg.org/doi/full/10.1190/geo2015-0387.1.
22. Marty, P, Boehm, C, & Fichtner, A. Shape optimization for transcranial ultrasound computed tomography | (2023) | Marty | Publications | Spie. in *SPIE Medical Imaging 2023* vol. 12470 77–88.